www.elsevier.nl/locate/ica

Inorganica Chimica Acta 312 (2001) 67–73

Inorganica Chimica Acta

Crystal structures and coordination-site exchange reactions of palladium(II) and platinum(II) complexes containing tris[2-(*tert*-butylthio)ethyl]amine

Kiyohiko Nakajima [a,*], Tomohiro Kajino [a], Matsuo Nonoyama [b], Masaaki Kojima [c]

[a] *Department of Chemistry, Aichi University of Education, Igaya, Kariya 448-8542, Japan*
[b] *Department of Chemistry, Graduate School of Science, Nagoya University, Chikusa, Nagoya 464-8602, Japan*
[c] *Department of Chemistry, Faculty of Science, Okayama University, Tsushima, Okayama 700-8530, Japan*

Received 8 July 2000; accepted 22 September 2000

Abstract

Palladium(II) and platinum(II) complexes, $[PdX(NS_3{}^1Bu)]BPh_4$ (X = Cl, Br, I; $NS_3{}^1Bu$ = tris[2-(*tert*-butylthio)ethyl]amine) and $[PtCl(NS_3{}^1Bu)]BPh_4$, were prepared, and their structures were determined by X-ray analyses. The geometry around the palladium and platinum atoms is square planar. The $NS_3{}^1Bu$ ligand functions as a tridentate ligand and one sulfur atom is not coordinated to the metal. The ^1H NMR spectrum of $[PdCl(NS_3{}^1Bu)]BPh_4$ in acetone-d_6 exhibited a dynamic behavior. At 20°C the spectrum showed a singlet signal at 1.60 ppm that can be assigned to *tert*-butyl protons, whereas at -70°C three singlet signals were observed at 1.36, 1.61, and 1.70 ppm with an intensity ratio of 1: 0.25: 2. The signals at 1.36 and 1.70 ppm are assigned to the *tert*-butyl protons in the square-planar structure, and these signals are consistent with the X-ray structure. The signal at 1.61 ppm can be assigned to the *tert*-butyl protons in a trigonal-bipyramidal structure where the three *tert*-butyl groups are magnetically equivalent. Thus, we concluded that the coordination-site exchange occurred via a trigonal-bipyramidal intermediate. The square-planar and trigonal-bipyramidal species of $[PdCl(NS_3{}^1Bu)]BPh_4$ are in equilibrium in acetone-d_6. The equilibrium was shifted toward the square-planar species on decreasing the temperature. The ^1H NMR spectra for $[PdX(NS_3{}^1Bu)]BPh_4$ (X = Cl, Br, and I) were similar to one another at the same temperature, suggesting that the site-exchange process is insensitive to the kind of coexisting halogen ligand. The site exchange reaction of $[PtCl(NS_3{}^1Bu)]BPh_4$ seems to occur more slowly than that of the palladium(II) analogue. © 2001 Elsevier Science B.V. All rights reserved.

Keywords: Variable-temperature ^1H NMR spectra; Palladium(II) complexes; Platinum(II) complexes; Square-planar structure; Trigonal-bipyramidal structure; Coordination-site exchange reaction; Five-coordinate intermediate

1. Introduction

A wide variety of square-planar d^8 metal complexes are known. Mechanisms for their substitution reaction have been extensively studied on the basis of their kinetic properties, and an associative mechanism has been proposed in many cases [1]. There is an interest in the geometry of the five-coordinate intermediate or the activated complex. It is not easy, however, to determine the structure of the intermediate directly. In order to study the mechanism of substitution reactions and to determine the geometries of transition states, ab initio calculations were applied to several square-planar platinum(II) and rhodium(I) complexes, and pseudo-trigonal-bipyramidal transition states were indicated [2].

In the coordination-site exchange reaction of the tripodal ligand in square-planar complexes, the five-coordinate trigonal-bipyramidal intermediate is presumed (Scheme 1). Tripodal ligands seem to stabilize trigonal-bipyramidal geometry. For example, $[NiX(NS_3{}^1Bu)]BPh_4$ ($NS_3{}^1Bu$ = tris[2-(*tert*-butylthio)ethyl]amine, X = Cl, Br, I) [3] was prepared, and the existence of a five-coordinate species was confirmed by the UV–vis spectra in the solid state and in solution. The UV–vis spectra of $[NiX(N_3P)]BPh_4$ (N_3P = bis(2-diethyl-

---

* Corresponding author. Tel.: +81-566-26 2355; fax: +81-566-26 2310.

E-mail address: knakajim@auccc.aichi-edu.ac.jp (K. Nakajima).

0020-1693/01/$ - see front matter

PII: S0020-1693(00)00333-9

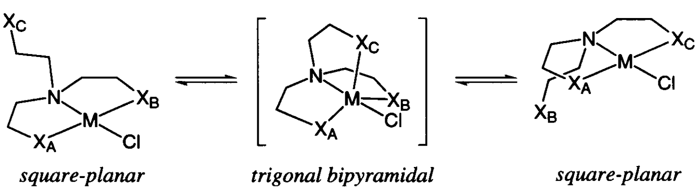

Scheme 1.

aminoethyl)(2-diphenylphosphinoethyl)amine, X = Cl, Br, I) [4] indicated that the square-planar and trigonal-bipyramidal species existed in equilibrium for X = Cl or Br, and for X = I, only the square-planar species was formed. Although, an equilibrium between the trigonal-bipyramidal and square-planar species of $[PdCl(trenMe_6)]^+$ ($trenMe_6$ = tris[2-(dimethylamino)ethyl]-amine) was suggested on the basis of the ^1H NMR spectra in solution [5], a detailed study has not been performed.

Thus, we are interested in the coordination-site exchange reaction of palladium(II) and platinum(II) complexes containing a tripodal ligand. The coordination-site exchange reaction rates for these complexes will be slower than those for the corresponding nickel(II) complex. Therefore, we expect that the five-coordinate intermediate may be detected as an isolated signal in the ^1H NMR spectra for palladium(II) and platinum(II) complexes.

In this work, we have used the tripodal ligand, tris[2-(*tert*-butylthio)ethyl]amine ($NS_3{}^tBu$), and prepared $[PdX(NS_3{}^tBu)]BPh_4$ (X = Cl, Br, I) and $[PtCl(NS_3{}^tBu)]BPh_4$. The structures of the complexes have been characterized by X-ray analyses, and the coordination-site exchange reaction of the ligand has been studied by the variable-temperature ^1H NMR spectra in the range 183–293 K.

2. Experimental

The tripodal ligand ($NS_3{}^tBu$) [6], $[PdCl_2(PhCN)_2]$ [7], and $[PtCl_2(cod)]$ (cod = 1,5-cyclooctadiene) [8] were prepared according to the literature procedures. $[PdBr_2(PhCN)_2]$ and $[PdI_2(PhCN)_2]$ were prepared in an approximately 30% yield by treating $[PdCl_2(PhCN)_2]$ in acetone with an excess amount of KBr and KI in water respectively. ^1H NMR spectra were measured at 400 MHz on a JEOL JNM LA-400 spectrometer with TMS as an internal reference.

2.1. Preparation of compounds

*2.1.1. $[PdCl(NS_3{}^tBu)]BPh_4$ (**1**)*

To an ethanol solution (20 cm^3) of $NS_3{}^tBu$ (0.039 g, 0.11 mmol) was added $[PdCl_2(PhCN)_2]$ (0.040 g, 0.10 mmol). The solution was refluxed for 10 min, and an ethanol solution (10 cm^3) of $NaBPh_4$ (0.035 g, 0.10 mmol) was added to give a yellow precipitate, which was filtered, washed three times with ethanol (3 × 10 cm^3), and dried. It was recrystallized by diffusion of hexane into an acetone solution of the complex at room temperature to yield yellow crystals. Yield 90%. *Anal.* Found: C, 61.13; H, 7.22; N, 1.84. Calc. for $[PdCl(NS_3{}^tBu)]BPh_4 = C_{42}H_{59}BClNPdS_3$: C, 61.01; H, 7.19; N, 1.69%. $PdCl_2$ and $[PdCl_2(cod)]$ were also used instead of $[PdCl_2(PhCN)_2]$ to give the same product, but the yields were lower.

*2.1.2. $[PdBr(NS_3{}^tBu)]BPh_4$ (**2**) and $[PdI(NS_3{}^tBu)]BPh_4$ (**3**)*

Complexes **2** and **3** were prepared according to the same procedure as that described for complex **1**, except that $[PdBr_2(PhCN)_2]$ and $[PdI_2(PhCN)_2]$ were used instead of $[PdCl_2(PhCN)_2]$ to yield orange and brown crystals respectively. Yield for **2** 93%. *Anal.* Found for **2**: C, 56.64; H, 6.74; N, 1.84. Calc. for $[PdBr(NS_3{}^tBu)]BPh_4 \cdot H_2O$[1] = $C_{42}H_{61}BBrNOPdS_3$ (**2**): C, 56.73; H, 6.91; N, 1.58%. Yield for **3** 73%. *Anal.* Found for **3**: C, 54.19; H, 6.54; N, 1.38. Calc. for $[PdI(NS_3{}^tBu)]BPh_4 = C_{42}H_{59}BINPdS_3$ (**3**): C, 54.94; H, 6.48; N, 1.53%.

*2.1.3. $[PtCl(NS_3{}^tBu)]BPh_4$ (**4**)*

To an ethanol solution (20 cm^3) of $NS_3{}^tBu$ (0.220 g, 0.60 mmol) was added $[PtCl_2(cod)]$ (0.188 g, 0.50 mmol). The solution was refluxed for 3 h, and an ethanol solution (10 cm^3) of $NaBPh_4$ (0.172 g, 0.50 mmol) was added to give a pale yellow precipitate, which was filtered, washed three times with ethanol (3 × 10 cm^3), and dried. It was recrystallized by diffusion of hexane into a solution of the complex in acetone at room temperature to yield pale yellow crystals. Yield 33%. *Anal.* Found: C, 54.77; H, 6.63; N, 1.64. Calc. for $[PtCl(NS_3{}^tBu)]BPh_4 = C_{42}H_{59}BClNPtS_3$: C, 55.10; H, 6.50; N, 1.53%.

---

[1] The elemental analysis suggested that complex **2** contains a water of crystallization; however, the water molecule was not found in the X-ray structure. The apparent discrepancy may be caused because these samples were taken from different batches.

2.2. Collection of X-ray data and structure determination

A summary of the crystallographic data and experimental details for complexes **1**, **2**, **3**, and **4** is given in Table 1. Single crystals of complexes **1** and **3** were mounted on glass fibers and the measurements were made on a Rigaku AFC7R four-circle diffractometer with graphite-monochromated Mo Kα radiation ($\lambda = 0.710\,69$ Å). Unit cell dimensions were determined by least-squares refinement of the best angular positions for 25 carefully centered reflections in the range $29.0 < 2\theta < 30.0°$ The data were collected using ω–2θ scan mode. The intensities of three standard reflections monitored after every 150 reflections remained constant throughout the data collection. Single crystals of complexes **2** and **4** were mounted on glass fibers and the measurements were made on a Rigaku RAXIS-RAPID diffractometer with graphite-monochromated Mo Kα radiation ($\lambda = 0.710\,69$ Å). A total of 44 images was collected with two different goniometer settings ($2\theta_{max} = 55°$). The camera radius was 127.40 mm. Exposure time was 5.00 min per degree. Readout was performed in the 0.100 mm pixel mode. For all the complexes, the diffraction data were processed by the PROCESS-AUTO program package. After removal of redundant data, a set of 4814 reflections for **1**, 7197 for **2**, 6548 for **3** ($I > 2\sigma(I)$), and 9697 for **4** (all observed unique data) were used for the structure determination. Absorption correction was applied based on ψ scan data for complex **1**, and by the numerical integration method from crystal shape for complex **3**. A numerical absorption correction using the program NUMABS [9] was applied for complexes **2** and **4**. The structures were solved by direct methods (SIR92 [10]) and expanded using Fourier techniques (DIRDIF94 [11]). All non-hydrogen atoms were refined anisotropically. Hydrogen atoms were placed at idealized positions and included in the refinement with fixed isotropic thermal parameters. All calculations were performed using the teXsan crystallographic software package [12] of Molecular Science Corporation.

3. Results and discussion

3.1. Structures of the complexes

The structures of complexes **1**, **2**, **3**, and **4** were almost the same as one another. Fig. 1 shows a perspective view of the complex cation, $[\mathrm{PdCl(NS_3{}^tBu)}]^+$ (**1**), representatively, and selected bond distances and angles are listed in Table 2 for all the complexes. The distances of Pd(1)–S(3) and Pt(1)–S(3) were 5.584(2) Å (averaged) and 5.604(2) Å respectively, and there was no bonding interaction. Thus, the coordination geometry around the palladium and platinum atoms is square planar, the donor atoms being the nitrogen, two sulfur, and halo-

Table 1
Crystallographic data and experimental details

Complex	**1**	**2**	**3**	**4**
Formula	$C_{42}H_{59}BClNPdS_3$	$C_{42}H_{59}BBrNPdS_3$	$C_{42}H_{59}BINPdS_3$	$C_{42}H_{59}BClNPtS_3$
M	826.78	871.23	918.23	915.47
Crystal system	triclinic	triclinic	triclinic	triclinic
Space group	$P\bar{1}$ (no. 2)	$P\bar{1}$ (no. 2)	$P\bar{1}$ (no. 2)	$P\bar{1}$ (no. 2)
a (Å)	14.595(8)	15.1625(5)	14.817(4)	15.1501(6)
b (Å)	15.276(7)	15.2824(4)	15.167(4)	15.2654(4)
c (Å)	11.980(5)	12.0159(4)	12.106(3)	12.0401(3)
α (°)	110.64(3)	110.6804(8)	109.35(2)	110.608(2)
β (°)	95.17(2)	109.8762(9)	96.54(2)	110.549(2)
γ (°)	116.51(4)	107.4746(9)	116.38(2)	106.681(2)
Z	2	2	2	2
V (Å^3)	2136(3)	2152.1(1)	2187(1)	2156.1(1)
μ(Mo Kα) (cm^{-1})	6.72	15.37	13.02	34.76
Transmission factor	0.93–1.00	0.82–0.92	0.66–0.88	0.48–0.57
Crystal color	yellow	orange	brown	pale yellow
D_{calcd} (g cm^{-3})	1.285	1.344	1.394	1.410
$2\theta_{max}$ (°)	50	55	55	55
R_1 (R)^a	0.031	0.043	0.048	0.050 (0.085)
R_w	0.048^b	0.064^b	0.061^b	0.137^c
S^d	1.53	1.25	1.61	1.82

[a] $R_1 = \Sigma||F_o| - |F_c||/\Sigma|F_o|$, R is obtained for all observed unique data.

[b] $R_w = [\Sigma w||F_o| - |F_c||^2/\Sigma w|F_o|^2]^{1/2}$.

[c] $R_w = [\Sigma w||F_o|^2 - |F_c|^2|^2/\Sigma w(|F_o|^2)^2]^{1/2}$.

[d] $S = [\Sigma w||F_o| - |F_c||^2/(m-n)]^{1/2}$ (m is the no. of reflections used; n is the no. of refined parameters).

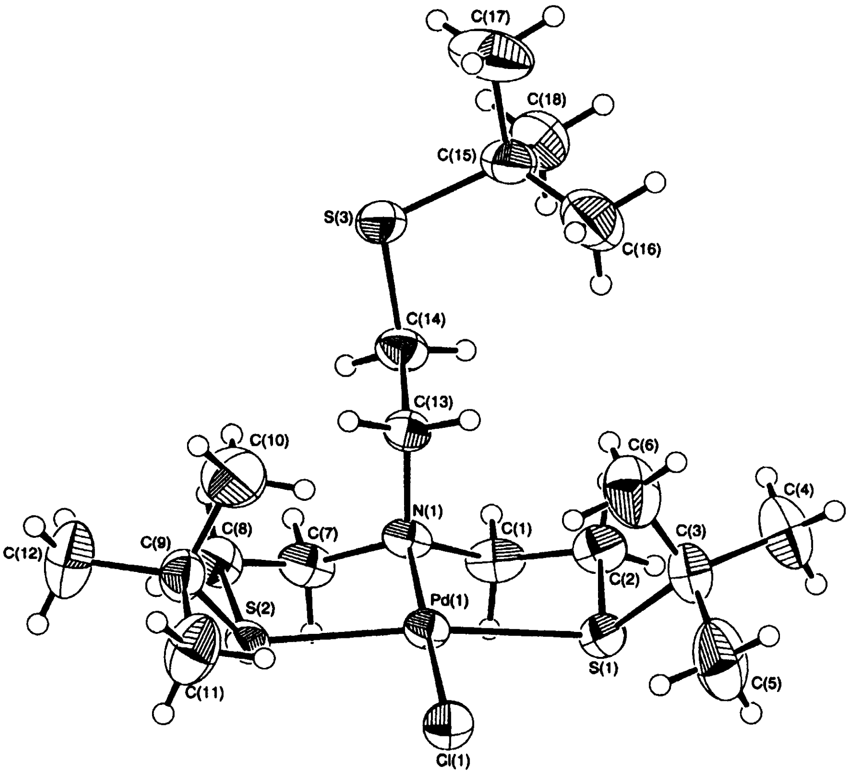

Fig. 1. Perspective ORTEP drawing of $[Pd(NS_3^tBu)Cl]^+$ cation in complex **1** with the atom labeling scheme. All non-hydrogen atoms are represented by their thermal displacement vibrational ellipsoids at 30% probability.

Table 2
Selected bond distances (Å) and bond angles (°)

	1 (M = Pd, X = Cl)	**2** (M = Pd, X = Br)	**3** (M = Pd, X = I)	**4** (M = Pt, X = Cl)
Bond distances				
M(1)–X(1)	2.3006(9)	2.4256(5)	2.5796(5)	2.312(2)
M(1)–S(1)	2.320(1)	2.321(1)	2.317(2)	2.301(2)
M(1)–S(2)	2.305(1)	2.303(1)	2.309(2)	2.288(2)
M(1)–N(1)	2.068(3)	2.079(3)	2.102(4)	2.097(5)
Bond angles				
X(1)–M(1)–S(1)	93.38(4)	93.33(3)	93.36(4)	93.24(6)
X(1)–M(1)–S(2)	93.06(4)	92.92(3)	92.60(4)	93.08(6)
X(1)–M(1)–N(1)	178.00(8)	177.68(8)	178.3(1)	178.4(1)
S(1)–M(1)–S(2)	166.67(4)	166.36(4)	166.15(6)	166.34(6)
S(1)–M(1)–N(1)	86.92(9)	86.9(1)	86.8(1)	87.1(2)
S(2)–M(1)–N(1)	87.05(9)	87.4(1)	87.6(1)	86.9(2)

gen atoms. The potentially tetradentate NS_3^tBu ligand is coordinated to the palladium and platinum atoms as a tridentate ligand having an uncoordinated pendant 2-(*tert*-butylthio)ethyl group. For example, no large deviation from a square-planar angle was observed at the palladium atom for complex **1**, but the chelate angles of S(1)–Pd(1)–N(1) (86.92(9)°) and S(2)–Pd(1)–N(1) (87.05(9)°) are slightly smaller than the bond angles of Cl(1)–Pd(1)–S(1) (93.38(4)°) and Cl(1)–Pd(1)–S(2) (93.06(4)°). The palladium and platinum atoms are displaced by 0.196(1) (averaged) and 0.192(1) Å toward the uncoordinated pendant arm from the least-squares plane defined by the four donor atoms. Although we cannot give a clear explanation for the displacement, it may reduce the steric repulsion among the two ^{t}Bu and uncoordinated pendant 2-(*tert*-butylthio)ethyl groups.

The bond length of Pd–X increases with respect to the X ligand in the order Cl (2.3006(9) Å) < Br (2.4256(5) Å) < I (2.5796(5) Å). These bond lengths are acceptable when the ionic radii for halogens and Pd^{2+} are taken into consideration. The bond length of Pd(1)–N(1) also increases with respect to the X ligand in the order Cl < Br < I, which is consistent with the order of trans influence of the X ligand as an electron donor toward Pd. The lengths of Pd–S(1) and Pd–S(2) and angles at the palladium atom are similar irrespective of the X ligand in complexes **1**, **2**, and **3**. It is notable that the averaged bond length of Pt(1)–S(1) and Pt(1)–S(2) (2.295(2) Å) is smaller than that of Pd(1)–S(1) and Pd(1)–S(2) (2.313(1) Å), although the Pt(1)–Cl(1) bond length (2.312(2) Å) is slightly larger than that for Pd(1)–Cl(1) (2.3006(9) Å). It seems that the sulfur atom has a strong affinity toward Pt(II).

Several complexes containing the NS_3^tBu ligand or its analogue have been prepared, and X-ray structure analysis was applied to some of them. The geometry around the metals of $[CoBr(NS_3^tBu)]PF_6$ [4], $[NiCl(NS_3^tBu)]BPh_4$ [13], and $[CuCl(NS_3Et)]ClO_4$ [14] was trigonal-bipyramidal in the solid state. It seems that the complexes of first-row transition metals with the NS_3R (R = alkyl; tris[2-(alkylthio)ethyl]amine) ligand prefer the trigonal-bipyramidal structure. However, the structures of $[NiX(NS_3Et)]BPh_4$ (X = Cl, Br, I) [4] were assigned to be octahedral in the solid state based on their reflectance spectra. The structure of $[HgCl(NS_3^iPr)]_2(Hg_2Cl_6)$ [15] has also been reported and the geometry around mercury was intermediate between a trigonal-bipyramid and a tetrahedron. Thus, the coordination mode of the NS_3R ligand depends upon the metal ion and the substituent on sulfur.

3.2. Coordination-site exchange reaction

The ^1H NMR spectrum of complex **1** in acetone-d_6 at room temperature showed a singlet at 1.60 ppm assignable to the *tert*-butyl protons. The ethylene protons were observed at 3.33 and 3.66 ppm, and the aromatic protons of BPh_4^- at 6.7–7.4 ppm. This spectrum is not consistent with the square-planar structure determined by X-ray analysis. Complex **1** has two kinds of *tert*-butyl group in the square-planar structure, i.e. the two *tert*-butyl groups on the coordinated sulfur atoms and the other one on the uncoordinated sulfur atom. Accordingly, a dynamic motion was suggested, and the ^1H NMR spectra were measured at low temperature. The variable-temperature ^1H NMR spectra of the *tert*-butyl signals are shown in Fig. 2. The singlet signal at 1.60 ppm (293 K) became broad with a decrease in temperature, and split into two broad signals (1.38 and 1.69 ppm) at 223 K. Another broad singlet signal emerged at 1.61 ppm at 203 K, and its intensity reduced at lower temperatures. The intensity ratio of the two signals at 1.70 and 1.36 ppm below 203 K was 2:1. We attributed these two signals to the *tert*-butyl protons on the coordinated and uncoordinated sulfur atoms of the square-planar complex as presented in Fig. 3(a), although the structure is not frozen even at 183 K. Holm and coworkers characterized the structure of $[NiCl(NS_3^tBu)]BPh_4$ by X-ray analysis to be trigonal-bipyramidal [13]. According to these results, we deduced that $[PdCl(NS_3^tBu)]^+$ is in equilibrium between the square-planar and trigonal-bipyramidal forms in acetone-d_6. Therefore, the signal at 1.61 ppm observed at low temperature (183–203 K) was assigned to the *tert*-butyl protons in the trigonal-bipyramidal structure (Fig. 3(b)), where three *tert*-butyl groups are magnetically equivalent. Thus, the trigonal-bipyramidal form has a sufficiently long lifetime to be detected by ^1H

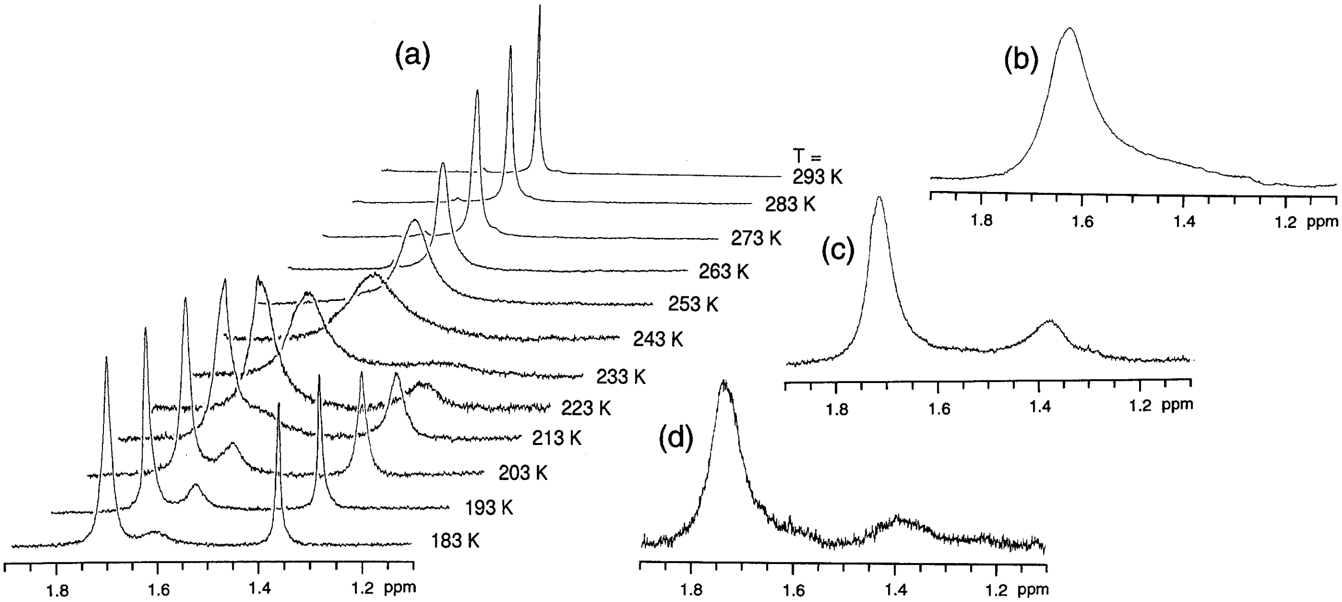

Fig. 2. Temperature-dependent ^1H NMR spectra due to the *tert*-butyl protons in acetone-d_6. (a) Complex **1** in the region of 183–293 K. (b) Complex **4** at 293 K. (c) Complex **2** at 223 K. (d) Complex **3** at 223 K.

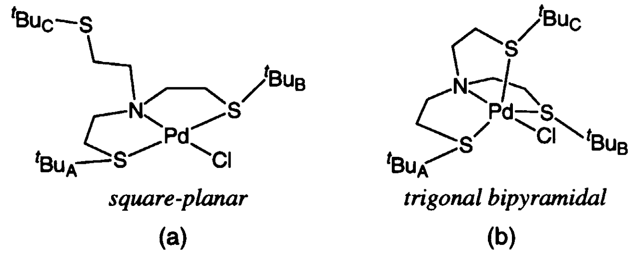

Fig. 3. Square-planar (a) and trigonal-bipyramidal (b) structures of complex **1**. In the trigonal-bipyramidal structure all three ^{t}Bu groups are magnetically equivalent, whereas in the square-planar structure the ^{t}Bu$_C$ group is not equivalent to the ^{t}Bu$_A$ and ^{t}Bu$_B$ groups.

NMR spectroscopy at low temperature (183–203 K). However, it seems that the inversion at the sulfur donor atoms is too fast to be observed even at 183 K. Accordingly, the singlet signal at 1.60 ppm observed at 293 K was interpreted as an averaged signal of the *tert*-butyl protons under the fast site-exchange conditions. This chemical shift (1.60 ppm) is very close to the weighted average (1.59 ppm) of the two signals (1.70 and 1.36 ppm).

The geometry around the nickel atom of [NiBr(N_3P)]BPh_4 was confirmed by an X-ray analysis to be square-planar in the solid state [3]. On the other hand, the UV–vis spectra of [NiX(N_3P)]BPh_4 (X = Cl, Br) indicated that both the diamagnetic square-planar and paramagnetic trigonal-bipyramidal species exist in equilibrium in solution. It seems that the structural characteristics of [NiX(N_3P)]BPh_4 (X = Cl, Br) are similar to those of complex **1** in the solid state and in solution. However, the signals of ^{1}H NMR spectra for [NiX(N_3P)]BPh_4 (X = Cl, Br) shifted continuously from the diamagnetic positions and at the same time became broader by decreasing the temperature. This means that the equilibrium between the square-planar and trigonal-bipyramidal species is shifted toward the latter on decreasing the temperature. On the contrary, in our case the relative ratio of the ^{1}H NMR signal intensities of the trigonal-bipyramidal species to that of the square-planar one decreased with a decrease in temperature. The stable form of complex **1** is a square-planar structure over the entire temperature region (183–293 K). Although the variable-temperature ^{1}H NMR spectra (Fig. 2(a)) were so complicated that we could not estimate the thermodynamic parameters, the resonances of the ^{1}H NMR spectra of *tert*-butyl protons for complexes **2** and **3** at 223 K resemble those of complex **1** very closely (Fig. 2). These results suggest that there is little difference in the rate of the coordination-site exchange reaction among these complexes. However, the resonance of the ^{1}H NMR spectrum for complex **4** at 293 K is similar to those of complexes **1**, **2**, and **3** at 243 K (Fig. 2). The coordination-site exchange reaction of complex **4** seems to occur more slowly than that of the analogous palladium(II) complex. The strong affinity of platinum toward sulfur, which is evidenced by the short Pt–S bond, may make a conformational change of complex **4** difficult.

4. Conclusions

We prepared palladium(II) and platinum(II) complexes containing tris[2-(*tert*-butylthio)ethyl]amine, and the structures were determined by X-ray analysis. The geometry around the palladium and platinum atoms was square planar in the solid state. However, the structure was not rigid and the coordination-site exchange reaction occurred in acetone-d_6. In this study, we could detect the five-coordinate intermediate of the reaction. The reaction proceeded via a trigonal-bipyramidal intermediate, which was identified by the variable-temperature ^{1}H NMR spectra. The variable-temperature NMR spectra of complex **1** can be interpreted as follows. (1) $T > 243$ K: the complex is stereochemically non-rigid, and fast site-exchange reaction occurs; (2) $203 < T < 243$ K: site-exchange rates are comparable to the NMR time scale; (3) $T < 203$ K: the complex exists mainly in a square-planar structure, but not frozen even at 183 K. The presence of a trigonal-bipyramidal intermediate was indicated.

5. Supplementary material

Tables of non-hydrogen atom coordinates and anisotropic thermal parameters, coordinates of the hydrogen atoms and bond lengths and angles have been deposited (nos 149231, 149232, 149233, and 149234 for complexes **1**, **2**, **3**, and **4** respectively) at the Cambridge Crystallographic Data Centre, 12 Union Road, Cambridge CB2 1EZ, UK (fax: +44-1223-336033; e-mail: deposit@ccdc.cam.ac.uk or www: http://www.ccdc.cam.ac.uk).

Acknowledgements

The present work was partially supported by a Grant-in Aid for Scientific Research No. 10640543 from the Ministry of Education, Science, and Culture. We express our thanks to the Institute for Molecular Science, Okazaki, for allowing the use of facilities for X-ray diffraction measurements.

References

[1] R.G. Wilkins, Kinetics and Mechanisms of Reaction of Transition Metal Complexes, 2nd edn, VCH, Weinheim, Germany, 1991.

[2] Z. Lin, M.B. Hall, Inorg. Chem. 30 (1991) 646.

[3] G. Fallani, R. Morassi, F. Zanobini, Inorg. Chim. Acta 12 (1975) 147.

[4] I. Bertini, P. Dapporto, G. Fallani, L. Sacconi, Inorg. Chem. 10 (1971) 1703.

[5] C.V. Senoff, Inorg. Chem. 17 (1978) 2320.

[6] R. Morassi, L. Sacconi, Inorg. Synth. 16 (1976) 174.

[7] J.R. Doyle, P.E. Slade, H.B. Jonassen, Inorg. Synth. 6 (1960) 218.

[8] J.X. McDermott, J.F. White, G.M. Whitesides, J. Am. Chem. Soc. 98 (1976) 6521.

[9] T. Higashi, Program for Absorption Correction, Rigaku Corporation, Tokyo, Japan, 1999.

[10] A. Altomare, M.C. Burla, M. Camalli, M. Cascarano, C. Giacovazzo, A. Guagliardi, G. Polidori, J. Appl. Crystallogr. 27 (1994) 435.

[11] P.T. Beurskens, G. Admiraal, G. Beurskens, W.P. Bosman, R. de Gelder, R. Israel, J.M.M. Smits, The DIRDIF-94 program system, Technical Report of the Crystallography Laboratory, University of Nijmegen, The Netherlands, 1994.

[12] Crystal Structure Analysis Package, Molecular Structure Corporation, 1985 and 1999.

[13] P. Stavropoulos, M.C. Muetterties, M. Carrié, R.H. Holm, J. Am. Chem. Soc. 113 (1991) 8485.

[14] E.A. Ambundo, M. Deydier, A.J. Grall, N. Aguera-Vega, L.T. Dressel, T.H. Cooper, M.J. Heeg, L.A. Ochrymowycz, D.B. Rorabacher, Inorg. Chem. 38 (1999) 4233.

[15] F. Cecconi, C.A. Ghilardi, S. Midollini, A. Orlandini, Inorg. Chim. Acta 269 (1998) 274.